

TIFR/TH/00-15

April, 2000

hep-ph/0003225

Study of R -parity-violating supersymmetric signals at an e^-e^- collider

Dilip Kumar Ghosh¹ and Sourov Roy²

*Department of Theoretical Physics, Tata Institute of Fundamental Research
Homi Bhabha Road
Mumbai - 400 005
INDIA*

Abstract

We study the pair production of right selectrons at a 500 GeV e^-e^- collider followed by their decay into an electron and a lightest neutralino. This lightest neutralino decays into multifermion final states in the presence of R -parity-violating couplings. A detailed analysis of possible signals is performed for some important regions of the parameter space. The signals are essentially free from the standard model backgrounds.

PACS NOS. : 12.60.Jv, 13.10.+q, 14.80.Ly

¹dghosh@theory.tifr.res.in

1 Introduction

Supersymmetry (SUSY), as one of the most attractive options beyond the standard model (SM), has been studied for the past few decades [1]. From the theoretical point of view it offers a solution to the hierarchy problem. On the other hand, a lot of effort has been devoted to looking at the phenomenological consequences of SUSY both in low-energy processes and at high-energy colliders [2]. One of the candidates for a realistic model is the minimal supersymmetric extension of the SM. In the SM, it is not possible to write down interactions which violate baryon number (B) or lepton number (L). In the SUSY version of the SM, particle spectrum is doubled and baryon number and lepton number are assigned to the supermultiplets, leading to $\Delta B = 1$ or $\Delta L = 1$ interactions in the Lagrangian. In the minimal supersymmetric standard model (MSSM) it is assumed that B and L are conserved quantum numbers. This is ensured by imposing a discrete multiplicative symmetry called R parity [3] which is defined as

$$R = (-1)^{L+3B+2S}$$

where S is the intrinsic spin of the particle.

It can be checked very easily that R equals +1 for standard model particles and -1 for the superpartners. An immediate consequence of R -parity conservation is that the sparticles appear in pair at each interaction vertex. This leads to the fact that the lightest supersymmetric particle (LSP) is stable. The interactions of the LSP must be of weak strength because they are mediated by virtual sparticles which are known to be quite heavy (of the order of the electroweak scale). The most favorite candidate to become an LSP is the lightest neutralino and the search strategies for supersymmetry guided by the principle of R -parity conservation are to look for signals with large missing energy and momentum carried by an undetected neutralino [2]. Also the LSP is a good candidate for the cold dark matter of the universe [4].

The conservation of R parity, however, is not prompted by any strong theoretical reason, and theories where R parity is violated through nonconservation of *either* B *or* L have been considered. Such scenarios can be studied by generalizing the MSSM superpotential to the following form [5]:

$$W = W_{MSSM} + W_{\mathcal{R}}, \tag{1}$$

with

$$W_{MSSM} = \mu \hat{H}_1 \hat{H}_2 + h_{ij}^l \hat{L}_i \hat{H}_1 \hat{E}_j^c + h_{ij}^d \hat{Q}_i \hat{H}_1 \hat{D}_j^c + h_{ij}^u \hat{Q}_i \hat{H}_2 \hat{U}_j^c \tag{2}$$

and

$$W_{\mathcal{R}} = \lambda_{ijk} \hat{L}_i \hat{L}_j \hat{E}_k^c + \lambda'_{ijk} \hat{L}_i \hat{Q}_j \hat{D}_k^c + \epsilon_i \hat{L}_i \hat{H}_2 + \lambda''_{ijk} \hat{U}_i^c \hat{D}_j^c \hat{D}_k^c. \tag{3}$$

Here, \hat{H}_1 , \hat{H}_2 are the SU(2) doublet Higgs superfields which give rise to the masses of down-type and up-type quark superfields, respectively, and \hat{L} (\hat{Q}) denote lepton (quark) doublet superfields. \hat{E}^c , \hat{D}^c , \hat{U}^c are the singlet lepton and quark superfields. i, j, k are the generational indices and we

have suppressed the SU(2) and SU(3) indices. The λ_{ijk} are antisymmetric in i and j while the λ''_{ijk} are antisymmetric in j and k . The first three terms in $W_{\mathcal{R}}$ violate lepton number and the last term violates baryon number. It is obvious that both the L and B violating terms cannot be present if the proton is stable. In order to get a large proton lifetime ($\sim 10^{40}$ s) [6] it is sufficient to demand that either L or B be violated which in turn breaks R parity. R -parity violation leads to considerable changes in the phenomenology. The most important consequence is that the LSP can decay now. Also, the lightest neutralino need not be the LSP because it is no longer a stable particle. The lepton number and baryon number violating terms mentioned above have received a lot of attention and constraints have been derived on these new couplings from present experimental data [7]. Prospects of R -parity violation have been studied in the context of following present and future colliders: CERN e^+e^- collider LEP, DESY ep collider HERA, $p\bar{p}$ at Fermilab Tevatron, CERN Large Hadron Collider (LHC), e^+e^- and $e\gamma$ Next Linear Collider (NLC) [8–10]. Here we investigate the signatures of R -parity breaking at future e^-e^- linear colliders. Our aim is to study the pair production of right selectrons (\tilde{e}_R) which will then decay into an electron and a neutralino. Finally the neutralino will decay into multifermions through different R -parity-violating couplings.

In this paper we shall discuss the R violation in three separate categories for the convenience of the analysis. We will consider, in turn, $W_{\mathcal{R}}$ with either the λ , λ' , or λ'' terms existing in the superpotential at a time. The bilinear term $\epsilon_i \hat{L}_i \hat{H}_2$ is also a viable agent for R -parity breaking which can induce vacuum expectation values for the sneutrino fields and generates a tree-level mass for one of the neutrinos [11, 12]. This scenario has been studied by several authors in the context of recent results from SuperKamiokande (SK) data on atmospheric neutrinos [13] and attempts have been made to find the correlation between the given pattern of neutrino masses and mixings and collider signatures of supersymmetry [14]. So far, no work has been reported which includes the study of R -parity violation through the bilinear term in the context of e^-e^- colliders and we wish to discuss it in our future work which requires a separate analysis altogether [15].

The paper is organized as follows. In Sec. 2, we describe the physics goals of e^-e^- colliders and their advantages and disadvantages from the point of view of a supersymmetry search. In Sec. 3 we will discuss the numerical results followed by our conclusions in Sec. 4.

2 Search for supersymmetry at e^-e^- collider

As we know, the current e^+e^- collider at LEP is at the verge of its closing. Apart from putting some lower bounds on different SUSY particles, there has been no sign of new physics beyond the SM from LEP. Perhaps one can hope to see some signals beyond the SM at run II of Tevatron and, of course, the LHC, but the clean environment of the next generation e^+e^- linear collider will definitely complement the signatures from hadron colliders. Even if SUSY is discovered at LHC, NLC can be used as a machine for precision measurements for different SUSY parameters [16].

Before going on to the discussion of the supersymmetry search, let us first mention in brief

the unique features of an e^-e^- collider which establishes its importance in order to make model independent measurements at future high-energy physics experiments [17]. First of all, it should be emphasized that at linear colliders the replacement of a beam of positrons with a beam of electrons can be achieved in a rather straightforward manner and can lead to the option of colliding electron beams.

At e^-e^- colliders, the initial energy is well known and both e^- beams can be highly polarized so that the initial states are specified. The backgrounds are, in general, extremely suppressed and they can be reduced further with specific choices of the beam polarizations. However, the total electric charge Q and total lepton number L of e^-e^- colliders forbid the pair production of most of the superpartners by virtue of total charge and lepton number conservation. This is one disadvantage of e^-e^- colliders where only selectrons can be pair produced through the exchange of a Majorana neutralino in the t and u channels [18, 19] as shown in Fig. 1. In contrast, at e^+e^- colliders, selectron pair production occurs through s -channel γ and Z exchange as well as through t -channel $\tilde{\chi}_i^0$ exchange. The interference between the s - and t -channel diagrams is always destructive for $\sqrt{s} > m_Z$ [20]. In the e^-e^- mode, since the u -channel diagram is present along with the t -channel diagram and the interference between them is constructive, the production cross section is always larger compared to the e^+e^- mode. This cross section can be further increased by choosing the initial electron beam polarization properly. It has been shown [19] that the right selectron pair production cross section is largest for the right-polarized initial electron beam. This can be explained from the fact that in most of the MSSM parameter space the LSP is B-ino dominated, which has a larger coupling with $e_R\tilde{e}_R$ compared to $e_L\tilde{e}_L$. Furthermore, it turns out that the selectron pair production cross section for the unpolarized initial state is smaller than that of right-polarized electron beams.

Another important feature of the e^-e^- collider is its behavior near threshold which shows a sharp rise in the selectron pair production cross section [21]. This enables one to measure the selectron masses very accurately. In contrast, at an e^+e^- collider the threshold measurement is rather poor, which compels one to determine the \tilde{e} mass (with an error of few GeV) from the measurement of the electron end point energy [21]. The study of slepton flavor violation can also be done very effectively in an e^-e^- collider.

In Fig. 2, we present contours for the cross section (in fb) for the production of $\tilde{e}_R^-\tilde{e}_R^-$ final states in the (μ, M_2) plane for $\tan\beta = 2, 20, 40$ and $\sqrt{s} = 500$ GeV. The mass of the right selectron is assumed to be 150 GeV for the plots in the left column and 200 GeV for the plots in the right column.

The explanation of the variation of cross section with the parameters which appear in the neutralino mass matrix, as shown in Fig. 2, is as follows. The area *ruled out by LEP-2* represents the region which is disallowed by the chargino search at LEP-2 and corresponds to a mass of the lighter chargino ($\tilde{\chi}_1^\pm$) less than 98 GeV [23]. This limit comes purely from kinematic considerations and does not depend on whether R parity is conserved or violated. The area which is marked as X

in the figure is not allowed because here the selectrons become lighter than the LSP and hence the selectron decaying to the lightest neutralino is forbidden ¹. Since we are considering right selectron pair production, the contribution to the cross section comes mainly from the lightest neutralino which is dominated by a B-ino over a large part of the parameter space. Here we assume the grand unified theory (GUT) relationship between the SU(2) and U(1) gaugino soft mass parameters M_2 and M_1 , $M_1 = \frac{5}{3} \tan^2 \theta_W M_2$. As the value of M_2 increases, the lightest neutralino starts becoming more and more B-ino dominated and hence the strength of the $e_R - \tilde{e}_R - \tilde{\chi}_1^0$ coupling increases at the same time. Also, the amplitude in this case requires a t -channel neutralino mass insertion. These two effects combined together lead to an increase in the cross section when M_2 is increased for a fixed value of μ [18]. This feature is evident from Fig. 2. For lower values of μ , the B-ino component in the lightest neutralino starts decreasing which means a fall in the cross section and hence in order to get the same cross section the value of M_2 (consequently the value of M_1) must be increased. With the increase in selectron mass the available phase space reduces and in order to get the same cross section as in the left column one must go to higher values of M_2 .

The decay of right selectron yields following final state:

$$e^- e^- \longrightarrow \tilde{e}_R^- \tilde{e}_R^- \longrightarrow e^- e^- \tilde{\chi}_1^0 \tilde{\chi}_1^0. \quad (4)$$

This will give rise to two like-sign electrons and large \cancel{p}_T signature. This kind of a signal as shown in Eq. (4) and the relevant backgrounds have been well studied [19].

In light of the above discussion, the next question which comes to mind is what could be the potential signatures at an $e^- e^-$ collider when R parity is violated. Recently, the effect of R parity violation has been studied for the production process $e_L^- e_R^- \longrightarrow \tilde{e}_L^- \tilde{e}_R^-$ [22]. In this work we will consider the pair production of right selectrons assuming 90% right-polarized electron beams because of the larger cross section in this case. The subsequent analysis will not depend on the choice of initial electron polarization. As we will see in the following section, since the lightest neutralino will decay, it will lead to multilepton final states with missing energy almost free from standard model backgrounds. However, right selectrons can also decay into heavier neutralino states, if it is allowed by kinematics. In that case, the cascade decays of heavier neutralino will produce more complex signals. For the simplicity of our analysis, we will not consider such decay patterns here.

3 Decay of $\tilde{\chi}_1^0$ and associated signals

In this section we will discuss the possible signatures arising from the decay of the LSP through different R -parity-violating interactions, through sfermion (sleptons and squarks) exchange diagrams. These Feynman diagrams and the amplitudes can be found in the literature [10, 24]. Here, we make

¹In R -parity-violating models, it is also possible that the *selectron*, rather than the lightest neutralino, is the LSP,

the assumption that of all the couplings which violate R parity, only one is dominant at a time, which is motivated from the fact that in the SM top quark Yukawa coupling is much larger than the others. Furthermore, we assume these couplings to be much smaller than the gauge couplings, though we require them to be large enough to make the LSP decay inside the detector. A generic R -parity-violating coupling should be larger than 10^{-5} to satisfy the above requirement [25, 7]. In our subsequent analysis we take these couplings in the range 10^{-1} - 10^{-2} . If the R -parity-violating operator is of the type LLE^c , the final states will have two charged leptons and a neutrino. The flavor of these leptons are determined by the type of λ_{ijk} coupling. If the R -parity-violating operator is of the type LQD^c , the final states will have either one charged lepton or a neutrino associated with two quarks. Finally in the presence of baryon number violating coupling $U^cD^cD^c$, the final state will have three quarks. Throughout this analysis we assume 250 GeV left-slepton mass [sneutrino mass is related to left-slepton mass through the SU(2) relation] and 500 GeV squark mass. All the squarks have been assumed to be degenerate in mass. In our parton level Monte Carlo analysis we treat quarks/partons as jets, and the direction of jets is same as that of the initial quarks/partons. We impose following selection criteria for these leptons and jets:

$$p_T^\ell > 5 \text{ GeV}, \quad |\eta_\ell| < 3, \quad (5)$$

$$p_T^j > 15 \text{ GeV}, \quad |\eta_j| < 3. \quad (6)$$

We merge two jets into a single jet if their angular separation $\Delta R_{jj} < 0.7$, where $(\Delta R_{jj})^2 \equiv (\Delta\eta)_{jj}^2 + (\Delta\phi_{jj})^2$, $\Delta\eta_{jj}$ and $\Delta\phi_{jj}$ being the difference of pseudorapidities and azimuthal angles, respectively, corresponding to two jets. The lepton is isolated from a jet if $\Delta R_{jl} > 0.4$, where ΔR_{jl} is defined in the same way as above.

3.1 Signals from λ -type couplings

Let us now discuss the signals which can be looked for when R parity is violated through the terms of the type λLLE^c . The pair-produced LSPs from the decay of the two right selectrons will lead to the final state consisting of $e^-e^- + 4\ell^\pm + \cancel{p}_T$. The flavor of the leptons coming from the neutralino decay will depend on the particular type of coupling involved. For example, λ_{123} coupling gives

$$\tilde{\chi}_1^0 \longrightarrow \nu_e \mu^- \tau^+, e^- \nu_\mu \tau^+, \bar{\nu}_e \mu^+ \tau^-, e^+ \bar{\nu}_\mu \tau^-, \quad (7)$$

with equal probabilities. Here, for simplicity we have considered a common value for all λ -type couplings taken to be $0.07(m_{\tilde{e}}/100 \text{ GeV})$, close to the existing indirect bounds relevant for most of those couplings. In order to tag the lepton flavor one must multiply the signal cross section with the efficiency of the corresponding lepton flavor identification.

Since there are two neutrinos in the final states, reconstructing the mass of the LSP in such a case is not possible. However, the kind of final state mentioned above is spectacular in the sense that it is free from standard model background and permits easy detection at a 500 GeV e^-e^-

In Fig. 3, we have shown the transverse momentum (p_T) distribution of the charged leptons produced in the final state for $M_{\tilde{e}_R} = 150$ GeV, and the following the set of input parameters $\mu = -450$ GeV, $M_2 = 200$ GeV and $\tan\beta = 2$. For this set of parameter points $M_{\tilde{\chi}_1^0} = 103$ GeV and $M_{\tilde{\chi}_2^0} = 206$ GeV. For later studies of the distributions we will use this set of input parameters. It is easy to see from this distribution that all six leptons survive the $p_T^\ell > 5$ GeV cut. Out of six leptons, two come from the decay of \tilde{e}_R ; the remaining four leptons come from the decay of $\tilde{\chi}_1^0$.

We display in Table 1, some representative values of the cross sections in order to get an idea about the strength of the signal. In obtaining these numbers, we required six leptons satisfying the criteria given in Eq. (5), and in addition imposed that $\cancel{p}_T > 15$ GeV. The \cancel{p}_T requirement ensures that the signal is SM background free. Two values of the right selectron mass, namely, $m_{\tilde{e}_R} = 150$ (GeV) and $m_{\tilde{e}_R} = 200$ (GeV), have been considered for the calculation of the cross sections. We have considered the actual branching ratios of the decays of right selectrons including the direct decays through R -parity-violating couplings as well as decays into heavier neutralinos. It has already been mentioned that if the decays into heavier neutralino states are allowed kinematically, they will lead to more complex signals which we have not considered in this work. For a fixed value of μ and $\tan\beta$, with increasing M_2 , the LSP mass increases; hence the MSSM decay of \tilde{e}_R decreases because of phase-space suppression, favoring the direct decay of \tilde{e}_R through R -parity-violating λ_{231} , which in turn reduces our signal. As is evident from this table, large cross sections may be obtained for a considerable region of the parameter space and with a projected integrated luminosity of 50 fb^{-1} at an e^-e^- collider one could see some thousands of events. It must be noted at this point that if taus are produced in the final state, they would decay mainly into hadrons, but that requires a separate analysis.

3.2 Signals from λ' -type couplings

The decay pattern of the LSP changes as we go on to the R -parity-violating couplings of the type $\lambda' LQD^c$. For example, λ'_{123} coupling gives

$$\tilde{\chi}_1^0 \longrightarrow \nu_e \bar{s} b, e^- c b, \bar{\nu}_e \bar{s} b, e^+ \bar{c} b. \quad (8)$$

As before, we again consider a common value for all λ' -type couplings. To identify the final state flavors one has to take into account the reduction in cross section due to flavor tagging efficiency. It should be mentioned at this point that unlike the λ case here all final states are not equiprobable. We categorize the signals in the following manner. All these states are assumed to be accompanied by two like-sign dielectrons arising from \tilde{e}_R decay: (1) $2\ell^\pm + \text{jets}$; both $\tilde{\chi}_1^0 \longrightarrow \ell^\pm jj$; (2) $\text{jets} + \cancel{p}_T$; both $\tilde{\chi}_1^0 \longrightarrow \nu jj$; (3) $\ell^\pm + \text{jets} + \cancel{p}_T$; one $\tilde{\chi}_1^0 \longrightarrow \ell^\pm jj$, the other $\tilde{\chi}_1^0 \longrightarrow \nu jj$.

The last channel will be enhanced by a combinatoric factor of 2. We have folded the cross section with the branching fraction of the LSP. The selection cuts (as discussed earlier) are applied to the leptons and jets. After the energy ordering ($E_{j_1} > E_{j_2} > E_{j_3} > E_{j_4}$), we study the jet p_T

arising from neutrinos for channels (2) and (3) listed above. The \cancel{p}_T distribution is shown in Fig. 5. The distribution a corresponds to the case when both the LSP decays into the νjj channel, where as b represents the \cancel{p}_T distribution when one of the LSP decays through the νjj mode and the other one through the $\ell^\pm jj$ mode.

Finally in Table 2 we give cross sections for signals for two \tilde{e}_R masses 150 GeV and 200 GeV. We required four jets and, respectively, four, three, or two leptons satisfying the criteria given in Eqs. (6) and (5), for channels (1), (2), and (3) listed above. In addition, $\cancel{p}_T > 15$ GeV is imposed for channels (2) and (3). Cross sections for heavier right-selectron mass ($= 200$ GeV) are lower than the corresponding quantities for 150 GeV \tilde{e}_R mass, just because of a lack of enough phase space. The difference in the three cross sections in each row can be explained from the branching ratio of $\tilde{\chi}_1^0$ in two different channels $\ell^\pm jj$ and νjj . The inputs remain same as in Table 1. The cross sections for these various channels are fairly large over a wide region of parameter space which is accessible in a 500 GeV e^-e^- collider. Signals corresponding to $e^-e^- + \text{jets} + \cancel{p}_T$ and $e^-e^- + \ell^\pm + \text{jets} + \cancel{p}_T$ final states may have the standard model background coming from W^-W^-ZZ production. But this cross section is found to be too low (< 40 fb) and does not affect the signal in a significant way.

If the produced LSP is highly relativistic, then its decay products will be confined within a narrow cone around the direction of the LSP. In that case, the lepton (decaying from LSP) in a particular hemisphere is identified and its invariant mass is constructed with all jets in the same hemisphere. A similar thing is done in the opposite hemisphere. Then we demand that these two invariant masses should lie within 10 GeV of each other. If these two invariant masses are equal or nearly equal, we can say that they arise from the same parent particle. In Fig. 6(a) we represent such an invariant mass distribution, which shows a distinct peak at the LSP mass ($= 103$ GeV). In order to get an estimate of the mass resolution, we have used Gaussian smearing [26] of the energies of jets and leptons to “mimic” the response of a detector:

$$\Delta E_j/E_j = 0.4/\sqrt{E_j} + 0.02, \quad \Delta E_l/E_l = 0.15/\sqrt{E_l} + 0.01. \quad (9)$$

In Fig. 6(b), we show the mass distribution after energy smearing. The LSP mass determined in this way has resolution $\Delta M/M = 4\%$. It should also be noted that for about 80% of the total events the mass reconstructed in both sides lies within 10 GeV of each other. In principle one can also reconstruct the selectron mass in this way, but a more precise determination can be done by a threshold scan [21].

3.3 Signals from λ'' -type couplings

Finally, the presence of λ'' in the superpotential can induce B number violating decay of the LSP. In this case, the LSP will simply decay into three hadronic jets:

where the sets of three jets have invariant mass peaking at the neutralino mass (assuming all jets are seen). As before, we impose the selection cuts on leptons and at least four jets. From the p_T distribution of six jets in Fig. 7 it is clear that for this value of the LSP mass ($= 103$ GeV), most of the jets are hard enough to satisfy the jet trigger requirement as discussed previously. From the jet number distributions in Fig. 8, we see that most of the time the cross section prefers to peak at the five-jet channel (44.69% of the events), followed by the six-jet (42.86% of the events) and four-jet (11.83% of the events) channels. The three-jet fraction of the cross section is less than 0.5%. Imposition of $p_T^j > 15$ GeV and $|\eta_j| < 3$ cuts on the jets reduces the jet number. Finally we also merge two jets into a single jet if their angular separation $\Delta R_{jj} < 0.7$. The probability of jet merging is highly dependent on the mass of the parent particle from which the jets originate and also on \sqrt{s} . The larger the boost of the parent particle, the higher the probability of jet merging. In this case, a 103 GeV LSP is produced from the decay of a 150 GeV right selectron. Each of these LSPs then decays into three jets with a reasonable boost, leading six jets to merge into five jets and occasionally into four and three jets.

In Table 3 we give signal cross sections for some representative values of parameters. In this case, we assume the squark mass to be 500 GeV, which enters as a propagator in the decay LSP. One can also reconstruct the LSP mass using the following strategy: selecting the hardest jet in the final state, its invariant mass is then constructed with all other jets in that hemisphere. A similar thing is done in the opposite hemisphere. Then we demand that these two invariant masses should lie within 10 GeV of each other. If these two invariant masses are equal or nearly equal, we can say that they arise from the same parent particle. Though we will not present here the invariant mass distribution, similar kinds of studies have been done by other authors and also by the ALEPH Collaboration in their study of the (now defunct) four-jet anomaly [9, 10, 27].

Before we conclude, we would like to mention the possible SM backgrounds in this case. We have earlier found that most of the time the signal cross section prefers to peak around five and six jets, free from any SM background. However, there is a small fraction of cross section that goes into four-jet channels, which is less important for our purpose as far as the SM backgrounds are concerned. This particular signal has SM backgrounds from (a) $e^-e^- \rightarrow e^-e^-ZZ$, (b) $e^-e^- \rightarrow e^-e^-Z^*Z$, and (c) $e^-e^- \rightarrow e^-e^-Z^*Z^*$, with hadronic decay of Z (assuming all jets are seen).

One can make a rough estimate for this background. After putting the selection cuts and including the relevant branching ratios the cross section for $e^-e^- \rightarrow e^-e^-Z$ is of the order of 100 fb. This cross section will get electroweak suppression if another Z boson is radiated; moreover, the $\text{Br.}(Z \rightarrow q\bar{q})$ will further reduce this. After all these, if this background is still comparable to the signal, then this can be eliminated by imposing the condition that the pair of dijet invariant mass M_{jj} should not peak around M_Z . However, this may reduce the signal cross section in the region of parameter space where the LSP mass is nearly degenerate with M_Z . The detailed calculation of the other two backgrounds [(b) and (c)] is very cumbersome and we will not perform this here. In this case, our main thrust will be to count the jets in the final state (associated with two electrons)

to distinguish it from the background.

4 Conclusions

We have discussed the pair production of right selectrons at a 500 GeV e^-e^- linear collider in the R -parity-violating supersymmetric model. The decay of right selectrons can yield a final state with an electron and a neutralino, mostly the LSP. Hence, we have two like-sign dielectrons and neutralinos in the final state. We have assumed that R parity is weakly violated and thus only the LSP will decay into multifermion states. Different possibilities have been considered and it seems that rather optimistic signals can be seen for this kind of model. The decay of the LSP gives charged leptons, jets, and neutrinos in the final state. The behavior of these leptons, jets, and missing transverse momentum (mainly due to neutrinos) has been analyzed using a parton level Monte Carlo event generator. This also enables us to study the approximate distributions for different kinematic variables of leptons and jets. The decay of the LSP through L -number-violating coupling (λ) leads to a very distinct signal with hard isolated leptons and large missing transverse momentum. There are no SM processes which can mimic this signal. Similarly, for λ'_{ijk} couplings, the signal basically consists of charged leptons, multiple jets, and/or missing transverse momentum. In addition to this, the Majorana nature of the LSP gives rise to like-sign dilepton signals with practically no SM backgrounds. It has been demonstrated that the reconstruction of the lepton-jet invariant mass can give a rough estimate for the LSP mass. For λ''_{ijk} coupling, the final state will have multiple jets associated with like-sign dielectrons. We have shown that proper jet counting is required to distinguish the signal from the SM backgrounds. In this case also it might be possible to determine the LSP mass from the jet invariant mass reconstruction.

Acknowledgments

The authors are grateful to Biswarup Mukhopadhyaya and Sreerup Raychaudhuri for helpful discussions.

References

- [1] For reviews, see, for example, H.P. Nilles, *Phys. Rep.* **110**, 1 (1984) ; H. Haber and G. Kane, *ibid.* **117**, 75 (1985); J.F. Gunion, in “Vancouver 1998, High energy physics”, Vol. 2, pp. 1684-1692, hep-ph/9810394.
- [2] See, for example, M. Carena *et al.*, *Rev. Mod. Phys.* **71**, 937 (1999), and references therein; also J.F. Grivaz, in *Supersymmetric Particle Searches at LEP in Perspectives on Supersymmetry*, edited by G.L. Kane (World Scientific, Singapore, 1997), pp. 179-203.
- [3] P. Fayet, *Phys. Lett.* **B69**, 489 (1977) ; G. Farrar and P. Fayet, *ibid.* **76B**, 575 (1978).
- [4] For a recent review, see N. Fornengo, University of Turin Report No. DFTT-18-98, 1998, astro-ph/9804295.
- [5] S. Weinberg, *Phys. Rev. D* **26**, 287 (1982) ; N. Sakai and T. Yanagida, *Nucl. Phys.* **B197**, 533 (1982) ; C. Aulakh and R. Mohapatra, *Phys. Lett.* **B119**, 136 (1983) .
- [6] Y. Totsuka, in *Proceedings of the XXIV Conference on High Energy Physics, Munich, 1988*, edited by R. Kotthaus and J.H. Kühn, (Springer-Verlag, Berlin, 1989); Icarus Detector Group at the International Symposium on Neutrino Astrophysics, Takayama, 1992.
- [7] H. Dreiner, in *An Introduction to Explicit R-Parity Violation in Perspectives on Supersymmetry*, edited by G.L. Kane (World Scientific, Singapore, 1998), pp. 462-479; R. Barbier *et al.*, “Report of the Group on the R-parity Violation”, hep-ph/9810232 (unpublished); G. Bhattacharyya, *Nucl. Phys. B (Proc. Suppl.)* **52 A**, 83 (1997) and references therein.
- [8] OPAL Collaboration, F. Abe *et al.*, *Phys. Rev. Lett.* **69**, 3439 (1992) ; ALEPH Collaboration, *Phys. Lett.* **B313**, 333 (1993) ; ALEPH Collaboration, *Phys. Lett.* **B349**, 238 (1995) ; H1 collaboration, S. Aid *et al.*, *Z. Phys.* **C71**, 211 (1996) ; H1 Collaboration, C. Adloff *et al.*, *Z. Phys.* **C74**, 191 (1997) ; ZEUS Collaboration, J. Breitweg *et al.*, *Z. Phys.* **C74**, 207 (1997) ; D.P. Roy, *Phys. Lett.* **B283**, 270 (1992) ; M. Guchait and D.P. Roy, *Phys. Rev. D* **54**, 3276 (1996) and *Phys. Rev. D* **57**, 4453 (1998) . D. Choudhury and S. Raychaudhuri, *Phys. Rev. D* **56**, 1778 (1997) ; F. Abe *et al.*, CDF Collaboration, *Phys. Rev. Lett.* **81**, 5278 (1998) ; R.M. Godbole *et al.*, *Nucl. Phys.* **B401**, 67 (1993) ; D.K. Ghosh *et al.*, *Phys. Lett.* **B396**, 177 (1997) ; D.K. Ghosh and S. Raychaudhuri, *Phys. Lett.* **B422**, 187 (1998) ; M. Chemtob, G. Moreau, *Phys. Rev. D* **59**, 055003 (1999) ; A. Datta and B. Mukhopadhyaya, *Phys. Rev. Lett.* **85**, 248 (2000).
- [9] D.K. Ghosh *et al.*, *Z. Phys.* **C75**, 357 (1997) .
- [10] D.K. Ghosh *et al.*, hep-ph/9904233.
- [11] L. J. Hall and M. Suzuki, *Nucl. Phys.* **B231**, 419 (1984) ; I-H. Lee, *Phys. Lett.* **B138**, 121 (1984) ; *Nucl. Phys.* **B246**, 120 (1984) ; S. Dawson, *Nucl. Phys.* **B261**, 297 (1985) . F. de Campos *et al.*, *Nucl. Phys.* **B451**, 3 (1995) ; M. Nowakowski and A. Pilaftsis, *Nucl. Phys.* **B461**, 19 (1996) ; J. W. F. Valle, hep-ph/9808292.
- [12] R. Hempfling, *Nucl. Phys.* **B478**, 3 (1996) ; H. P. Nilles and N. Polonsky, *Nucl. Phys.* **B484**, 33 (1997) ;

- and B. Mukhopadhyaya, *Phys. Rev. D* **55**, 7020 (1997) ; M. A. Díaz *et al.*, *Nucl. Phys.* **B524**, 23 (1998) ; E. J. Chun *et al.*, *Nucl. Phys.* **B544**, 89 (1999) ; M. Hirsch *et al.*, hep-ph/0004115.
- [13] Y. Fukuda *et al.*, *Phys. Lett.* **B433**, 9 (1998) ; *Phys. Rev. Lett.* **81**, 1562 (1998) .
- [14] V. Bednyakov *et al.*, *Phys. Lett.* **B442**, 203 (1998) ; B. Mukhopadhyaya *et al.*, *Phys. Lett.* **B443**, 191 (1998) ; A. Datta *et al.*, *Phys. Rev. D* **61**, 055006 (2000) ; E. J. Chun and J. S. Lee, *Phys. Rev. D* **60**, 075006 (1999) ; S. Y. Choi *et al.*, *Phys. Rev. D* **60**, 075002 (1999) .
- [15] D. K. Ghosh and S. Roy *Work in progress.*
- [16] M.E. Peskin and H. Murayama, *Ann. Rev. Nucl. Part. Sci.* **46**, 533 (1996); E. Accomando *et al.*, *Phys. Rep.* **299**, 1 (1998) and references therein.
- [17] *Proceedings of the Electron-Electron Linear Collider Workshop*, edited by C.A. Heusch, *Int. J. Mod. Phys.* **A13**, 2383 (1998) .
- [18] W.Y. Keung and L. Littenberg, *Phys. Rev. D* **28**, 1067 (1983) .
- [19] F. Cuypers *et al.*, *Nucl. Phys.* **B409**, 128 (1993) .
- [20] A. Bartl *et al.*, *Z. Phys.* **C34**, 411 (1987) .
- [21] J.L. Feng in [17].
- [22] U. Mahanta, *Phys. Rev. D* **61**, 035006 (2000).
- [23] ALEPH Collaboration, F. Cerutti *et al.*, hep-ex/9910031; L3 Collaboration, M. Acciarri *et al.*, *Phys. Lett.* **B472**, 420 (2000).
- [24] J. Butterworth and H. Dreiner, *Nucl. Phys.* **B397**, 3 (1997) ; E.A. Baltz and P. Gondolo, *Phys. Rev. D* **57**, 2969 (1998) .
- [25] See, S. Dawson in Ref. [11].
- [26] See, M.E. Peskin and H. Murayama in Ref. [16].
- [27] ALEPH Collaboration, R. Barate *et al.*, *Phys. Lett.* **B420**, 196 (1998) .

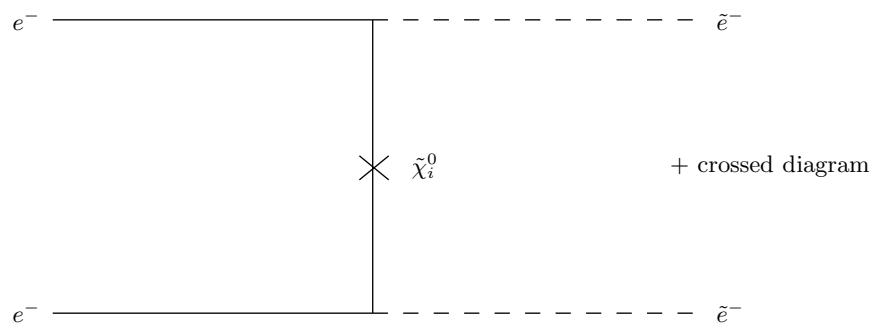


Figure 1: Feynman diagram for $e^-e^- \rightarrow \tilde{e}^-\tilde{e}^-$.

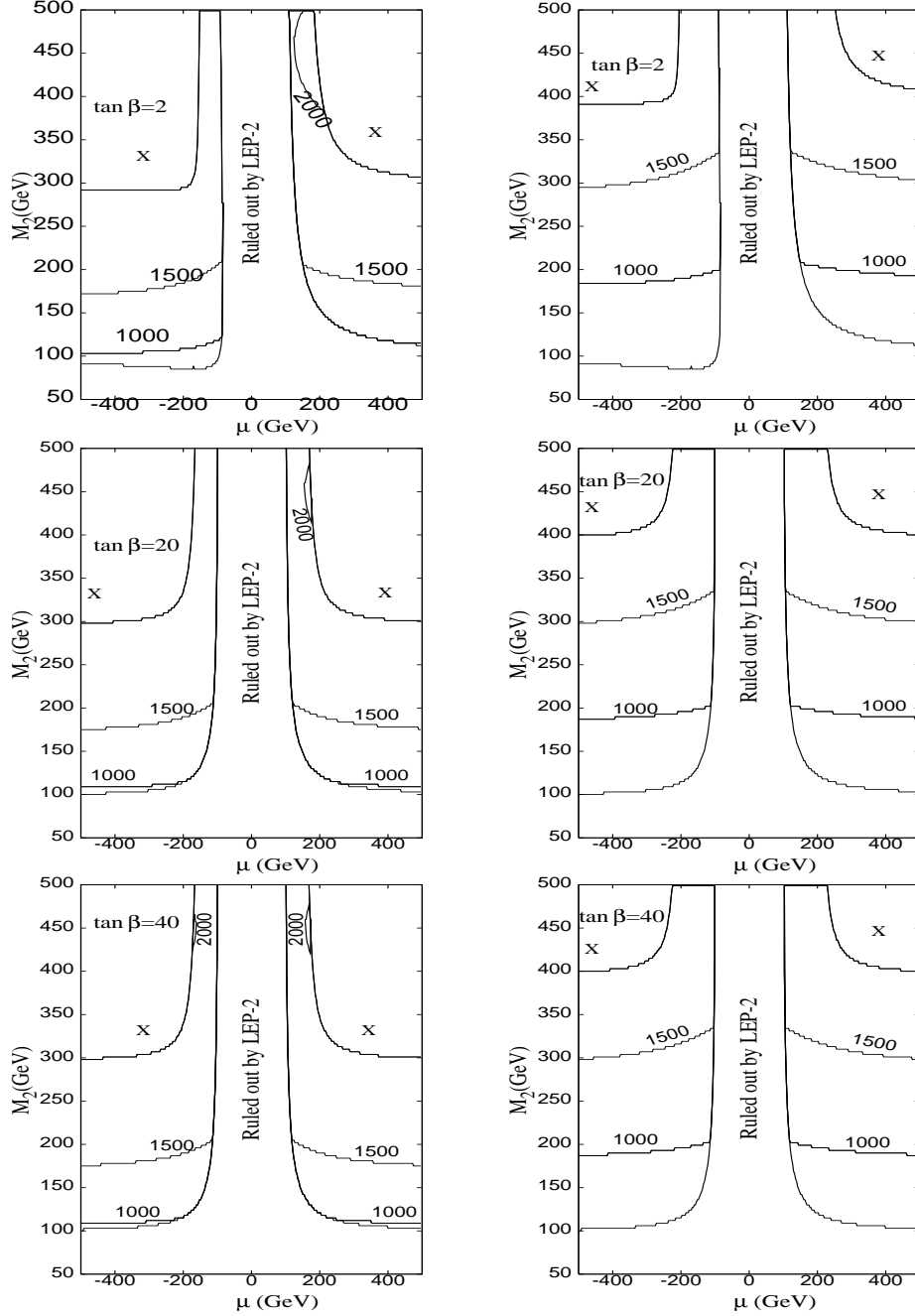


Figure 2: Contours of cross section (in fb) for production of a pair of right selectrons at an e^-e^- collider with right-polarized (90%) electron beams. The left and right columns correspond to 150 GeV and 200 GeV right selectron masses.

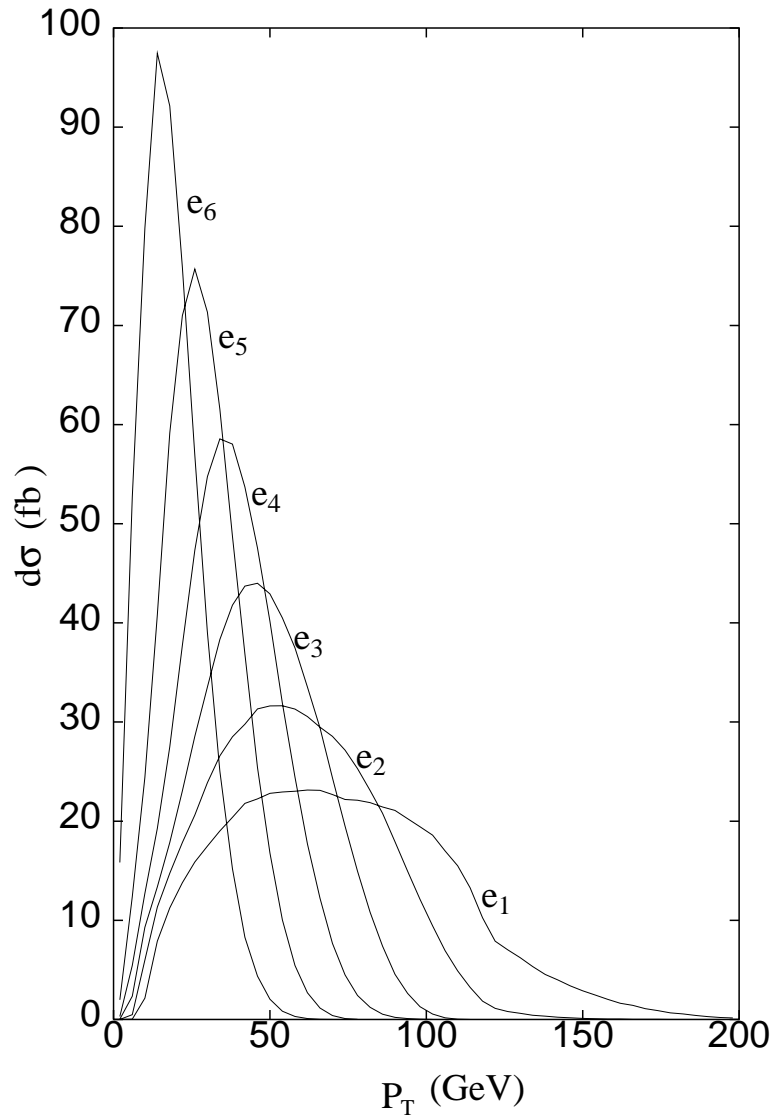


Figure 3: p_T distribution of leptons for the λ_{ijk} case. The MSSM input parameters are $\mu = -450$ (GeV), $M_2 = 200$ (GeV), and $\tan\beta = 2$. The number adjacent to each curve represents leptons with the following energy ordering: $E_{\ell_1} > E_{\ell_2} > E_{\ell_3} > E_{\ell_4} > E_{\ell_5} > E_{\ell_6}$.

				$m_{\tilde{e}_R} = 150$ (GeV)	$m_{\tilde{e}_R} = 200$ (GeV)
μ (GeV)	M_2 (GeV)	$\tan \beta$	$m_{\tilde{\chi}_1^0}$ (GeV)	σ (fb)	σ (fb)
-450	200	2	103.1	537.40	407.0
-375	250	2	128.4	163.22	380.86
400	250	2	118.9	334.86	410.11
-500	280	20	140.2	11.93	325.05
375	200	20	98.5	564.31	398.30
475	265	20	131.6	107.16	372.35
-480	300	40	149.8	0.0	252.30
-350	225	40	111.5	448.23	413.10
400	200	40	99.0	563.24	400.41

Table 1: Signal ($e^-e^- + 4\ell^\pm + \cancel{p}_T$) cross section assuming LSP decays through λ_{ij1} coupling for some representative values of the input parameters. For λ_{ijk} with $k \neq 1$, these cross sections would be larger by at least a factor of 2 since, in that case, the \tilde{e}_R only has R -parity-conserving decay modes.

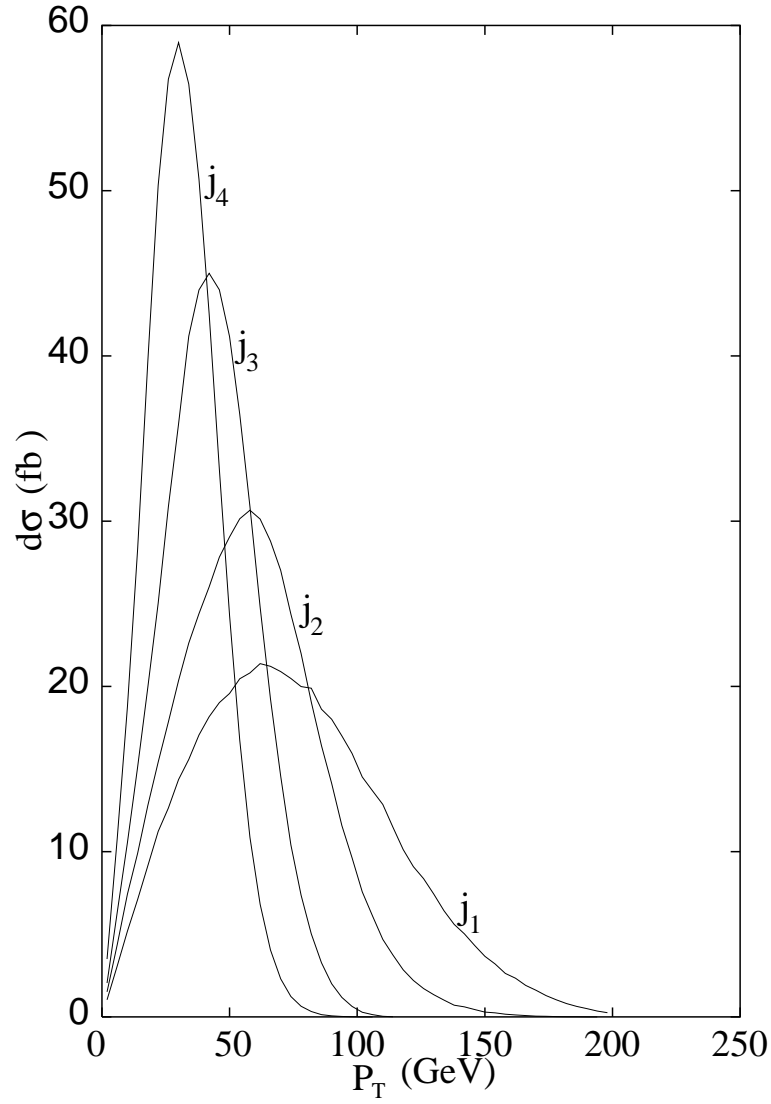


Figure 4: p_T distribution of jets for both $\tilde{\chi}_1^0 \rightarrow \ell^\pm jj$ channels through λ'_{ijk} coupling. The number adjacent to each curve represents jets with the following energy ordering: $E_{j_1} > E_{j_2} > E_{j_3} > E_{j_4}$. The input parameters are same as in Fig. 3.

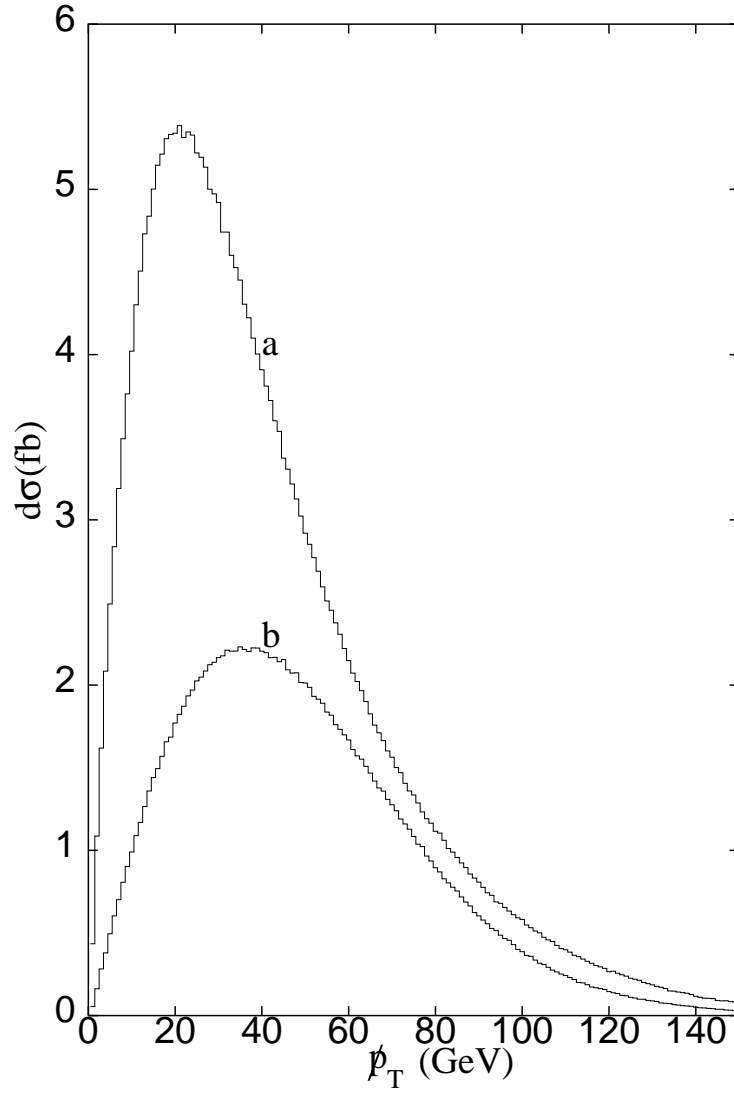


Figure 5: p_T distribution for the λ'_{ijk} case. *a*: both $\tilde{\chi}_1^0 \rightarrow \nu jj$. *b*: one $\tilde{\chi}_1^0 \rightarrow \ell^\pm jj$, the other one $\tilde{\chi}_1^0 \rightarrow \nu jj$. The input parameters are same as in Fig. 3.

				$m_{\tilde{e}_R} = 150$ (GeV)	$m_{\tilde{e}_R} = 200$ (GeV)
μ (GeV)	M_2 (GeV)	$\tan \beta$	$m_{\tilde{\chi}_1^0}$ (GeV)	σ (fb)	σ (fb)
-450	200	2	103.1	184.40	130.01
				214.54	150.20
				126.85	89.43
-375	250	2	128.4	234.20	180.47
				322.0	245.66
				180.80	137.70
400	250	2	118.9	58.68	43.46
				239.80	175.72
				137.00	100.50
-500	280	20	140.2	120.26	125.81
				277.60	289.10
				152.91	158.83
375	200	20	98.5	73.95	51.71
				184.42	128.8
				110.64	77.31
475	265	20	131.6	126.84	100.50
				321.33	253.00
				179.23	140.38
-480	300	40	149.8	2.79	130.48
				7.23	320.20
				4.25	173.53
-350	225	40	111.5	101.20	72.85
				246.40	176.07
				142.30	102.0
400	200	40	99.0	82.48	57.60
				190.30	132.70
				114.06	79.80

Table 2: Signal cross section assuming LSP decays through λ'_{ijk} coupling for some representative

values of the input parameters. In each row, the first, second, and third numbers correspond to

cross sections for the following final states: $e^-e^- + 2\ell + \cancel{\chi}$, $e^-e^- + \ell + \cancel{\chi}$, and $e^-e^- + \text{ jets} + \cancel{\chi}$.

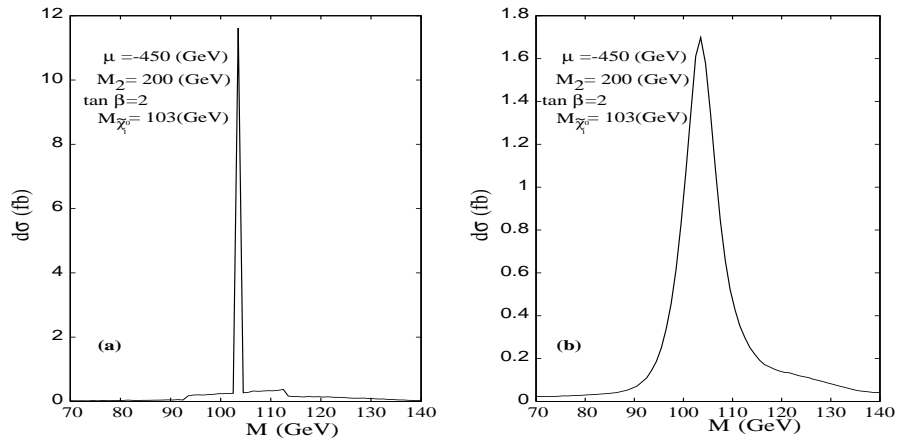


Figure 6: Distribution in invariant mass reconstruction from the lepton and all jets in the same hemisphere. (a) without lepton and jet energy smearing and (b) with lepton and jet energy smearing. Both $\tilde{\chi}_1^0$ decay into the $\ell^\pm jj$ channel through λ'_{ijk} coupling.

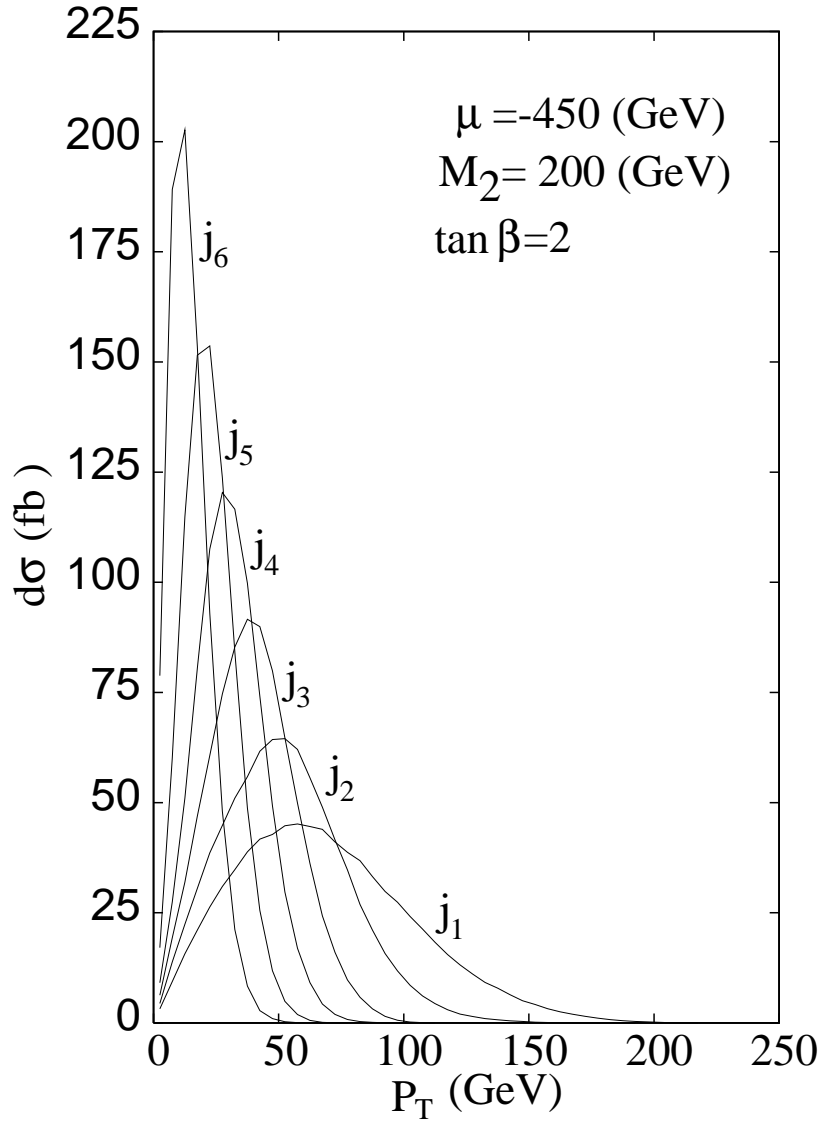


Figure 7: p_T distribution of jets for the λ''_{ijk} case. The number adjacent to each curve represents jets with the following energy ordering: $E_{j_1} > E_{j_2} > E_{j_3} > E_{j_4} > E_{j_5} > E_{j_6}$.

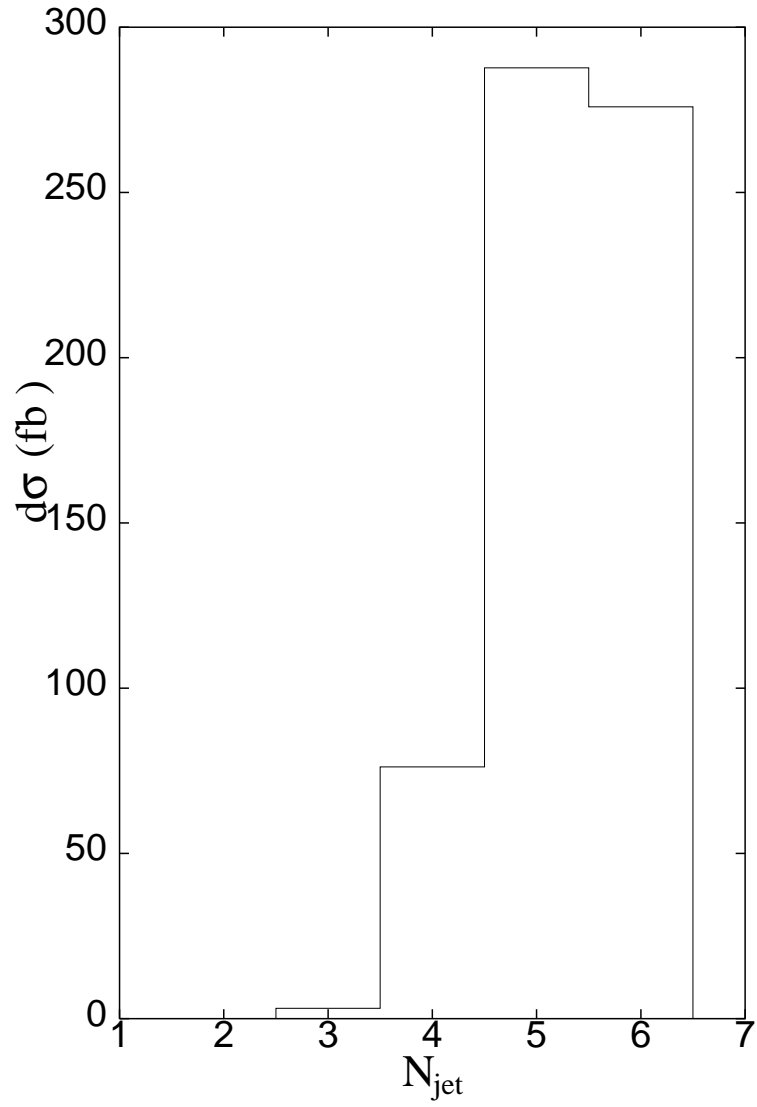


Figure 8: Number of jets (N_{jet}) when $\tilde{\chi}_1^0 \rightarrow jjj$ through λ''_{ijk} coupling.

				$m_{\tilde{e}_R} = 150$ (GeV)	$m_{\tilde{e}_R} = 200$ (GeV)
μ (GeV)	M_2 (GeV)	$\tan \beta$	$m_{\tilde{\chi}_1^0}$ (GeV)	σ (fb)	σ (fb)
-450	200	2	103.1	645.65	447.14
-375	250	2	128.4	925.61	714.22
400	250	2	118.9	859.80	634.50
-500	280	20	140.2	803.53	842.07
375	200	20	98.5	588.11	404.50
475	265	20	131.6	953.10	758.86
-480	300	40	149.8	45.0	929.10
-350	225	40	111.5	758.20	540.92
400	200	40	99.0	595.21	409.54

Table 3: Signal ($e^-e^- + \text{jets}$) cross section assuming LSP decays through λ''_{ijk} coupling for some representative values of the input parameters.